Journal of Organometallic Chemistry 696 (2011) 544–550

Contents lists available at ScienceDirect

Journal of Organometallic Chemistry

journal homepage: www.elsevier.com/locate/jorganchem

# Synthesis of siloxane-based PAMAM dendrimers and luminescent properties of their lanthanide complexes

Yuzhong Niu [a,b], Haifeng Lu [a], Dengxu Wang [a], Yuanzhi Yue [a], Shengyu Feng [a,*]

[a] Key Laboratory of Special Functional Aggregated Materials of Ministry of Education, School of Chemistry and Chemical Engineering, Shandong University, Jinan 250100, PR China
[b] School of Chemistry and Materials Science, Ludong University, Yantai 264025, PR China

ARTICLE INFO

*Article history:*
Received 12 July 2010
Received in revised form
26 August 2010
Accepted 7 September 2010
Available online 21 September 2010

*Keywords:*
Synthesis
Siloxane
PAMAM dendrimers
Luminescent properties
Lanthanide complexes

ABSTRACT

The 0.5–2 generations of siloxane-based PAMAM dendrimers with 1, 3-bis(3-aminopropyl) tetramethyldisiloxane (G0) as core unit were synthesized by two different methods. Their structures were characterized by FTIR, $^{1}$H NMR, $^{13}$C NMR, LC/MS, TGA, and DSC. Results show that method two is more suitable as its synthetic procedure is simple and it provides higher yield than method one. DSC analysis indicates that the introduction of the siloxane linkage into the interior of the dendrimers has significant effect on the flexibility of the dendrimer structures. Lanthanide complexes of the newly designed siloxane-based PAMAM dendrimers were obtained by complexing with Eu(III) and Tb(III), respectively. The luminescent properties of the complexes in the solution were investigated. Narrow-width red and green emissions were observed from the complexes of G0.5, G1.5, and G2.0, indicating intramolecular energy transfer process takes place between ligands and lanthanide ions.



## 1. Introduction

Luminescent lanthanide complexes have attracted considerable attentions for their excellent emission properties such as long luminescence lifetime, photostability, and narrow emission bandwidths [1–4]. These properties make them promising candidates for a wide variety of biological applications, including drug discovery, biochemical sensors, medical diagnostics, and fluoroimmuno-assays [5–8]. Especially europium (III) and terbium (III) complexes, which show luminescence in the visible region, have been extensively investigated [6–11].

In general, excellent luminescence properties of lanthanide complexes are attributed to the energy transfer from ligands to lanthanide ions, that is, the intense lanthanide ion luminescence originates from the intramolecular energy transfer from the excited state of the ligand to the emitting level of lanthanide ion, which is known as “antenna effect” [12–14]. In recent years, considerable efforts have been devoted to the design of suitable ligands which can efficiently optimize the luminescent properties of lanthanide ions for their biological applications. A promising strategy is to incorporate the chromophores into a multidentate chelating ligand containing carbonyl or amide groups with strong binding abilities to lanthanide ions [15–18].

Dendrimers are hyperbranched polymers with well-defined geometries and surface functionality [19–21]. Polyamidoamine (PAMAM) dendrimers have drawn considerable interest for their potential biological applications in drug delivery, gene transfection, and imaging [22–26]. These macromolecules can also be functionalized to incorporate transition metal complexes into the dendrimer backbone. PAMAM dendrimers, whose branches contain internal carbonyl and amide groups, are promising candidates for luminescent materials [10]. However, with the increasing of the generation, the increased steric hindrance at the dendrimer periphery make it hard for metal ions to diffuse into the interior of the dendrimer, which will affect the binding abilities of PAMAM dendrimers for lanthanide ions [22,27,28]. Therefore, the design and synthesis of PAMAM dendrimers based on novel cores to alleviate the surface congestion in higher generation, will facilitate the binding of lanthanide ions more efficiently and promote their applications in biological systems. It is particularly interesting to note that siloxane-based compounds, which exhibit unique properties such as excellent biocompatibility, high degree of flexibility, and an exceptionally low glass transition temperature, have a remarkable effect on supramolecular geometry [29–32]. The incorporation of siloxane into the interior of PAMAM dendrimers may dramatically alter the morphology and properties of these compounds by making the overall morphology less compact, and thus allowing the access of lanthanide ions to the internal carbonyl and amide groups more easily even at larger generations.

* Corresponding author. Tel.: +86 531 88364866; fax: +86 531 88564464.
*E-mail address:* fsy@sdu.edu.cn (S. Feng).

0022-328X/$ – see front matter © 2010 Elsevier B.V. All rights reserved.
doi:10.1016/j.jorganchem.2010.09.022

In the present study, we described the synthesis of the 0.5–2 generations PAMAM dendrimers with 1, 3-bis(3-aminopropyl) tetramethyldisiloxane (G0) as core unit by two different methods according to the procedure described in Scheme 1. Their structures were fully characterized by FTIR, $^1$H NMR, $^{13}$C NMR, LC/MS, TGA, and DSC. The newly designed siloxane-based PAMAM dendrimers were then complexed with Eu(III) and Tb(III) to form lanthanide complexes, and their luminescent properties in solution were investigated.

## 2. Experimental

### 2.1. Materials and methods

Fourier transform infrared spectra (FTIR) were recorded on a Bruker Tensor 27 spectrophotometer (Bruker, Switzerland). Test conditions: potassium bromide pellets, 32 scans, resolution: 4 cm$^{-1}$. The data were treated with OPUS spectroscopy software of version 6. $^1$H NMR and $^{13}$C NMR were measured in chloroform on a Bruker AVANCE-400 NMR Spectrometer, and chemical shifts were recorded in parts per million (ppm) without internal reference. Molecular weights were determined by Aglient HP1100 LC-Applied Biosystems API4000 TQ Mass Spectrometer (LC/MS). Thermal characteristics of the samples were determined with thermogravimetric analyzer (TGA) and different scanning calorimeter (DSC). TGA was performed with a MettlerToledo SDTA-854 TGA system. The analysis was performed with approximately 10 mg of samples in a dynamic nitrogen atmosphere (flow rate 50 ml/min) at a heating rate of 10 °C/min. DSC measurements were carried out in MettlerToledo DSC822 series. About 40 mg sample pan was ramped from −100 to 100 °C at the rate of 10 °C/min in a steady flow of nitrogen (20 ml/min). The fluorescence spectra were determined with ISS K2-Digital spectrophotometer: excitation slit width = 10 nm, emission slit width = 3 nm.

Methyl acrylate (MA), ethylenediamine (EDA), allylamine (AA), hexamethyl disilizane ($MM^N$), 1,1,3,3-tetramethyldisiloxane ($M^HM^H$), tetrahydrofuran (THF) were redistilled just before use. Europium and terbium nitrates were obtained from their corresponding oxides in dilute nitric acid. All of the other reagents used were of analytical-regent grade.

### 2.2. Preparation of allylaminotrimethylsilane (ATMS)

ATMS was prepared according to the procedure described in references [33,34]. A suspension of 11.40 g AA (0.2 mol), 19.34 g (0.12 mol) of $MM^N$ and 0.07 g anhydrous $(NH_4)_2SO_4$ was charged into a 100 ml flask. The reaction mixture was heated under argon

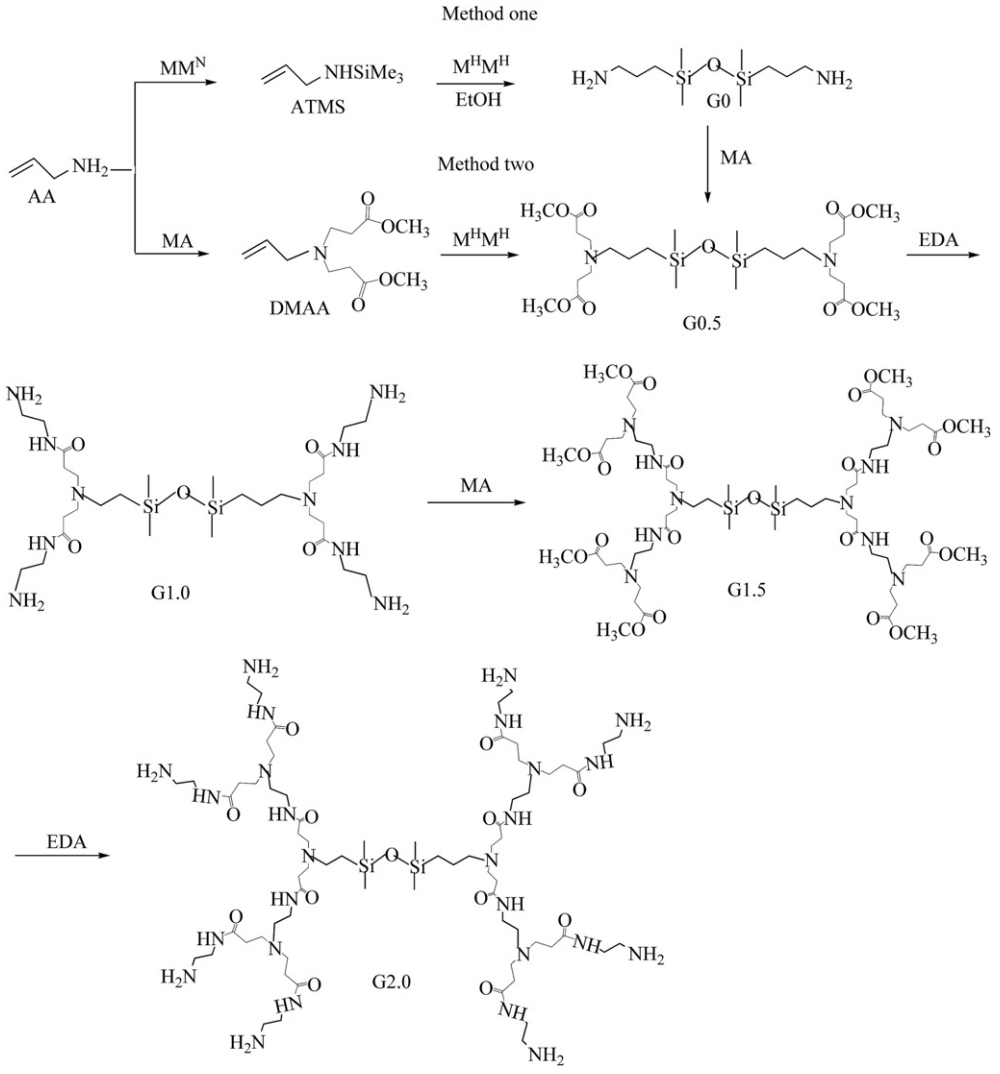


**Scheme 1.** The synthetic routes of siloxane-based PAMAM dendrimers.

atmosphere and refluxed over night until the temperature reached 106 °C. Then the reaction mixture was cooled to room temperature and the precipitate was filtered off. The liquid mixture was distilled and 18.83 g (0.15 mol) ATMS was obtained. (Yield: 73%). b.p. 110–112 °C (b.p. = 110–112 °C in Ref. [34]).

### 2.3. Preparation of DMAA

DMAA was prepared by Michael addition reaction of MA with AA according to the procedure described elsewhere [27]. Under argon atmosphere, a mixture of 2.85 g (0.05 mol) AA and 12.90 g MA (0.15 mol) in 70 ml of methanol was stirred at 50 °C for 36 h. Then the solvent and excess MA was removed under reduced pressure at 50 °C using a rotary evaporator, and 11.45 g (0.05 mol) DMAA was obtained. (Yield: 100%). $^1$H NMR ($CDCl_3$): $\delta$ (ppm) 2.38–2.42 (t, 4H, $NCH_2CH_2CO$), 2.72–2.75 (t, 4H, $NCH_2CH_2CO$), 3.04–3.06 (d, 2H, $CH_2$=$CHCH_2N$), 3.62 (s, 6H, $OCH_3$), 5.07–5.15 (t, 2H, $CH_2$=$CHCH_2N$), 5.70–5.80 (m, 1H, $CH_2$=$CHCH_2N$).

### 2.4. Preparation of G0

Similar to the method described in Ref. [35], a suspension of 15.48 g (0.12 mol) ATMS and three drops of Karstedt catalyst was added into the flask under argon atmosphere. The mixture was heated to 95 °C and then 6.7 g (0.05mol) $M^HM^H$ was added dropwise into the flask. After the reaction was initiated, the temperature of the mixture was maintained between 110 °C and 125 °C. When the reaction was complete, 30 ml of anhydrous ethanol was added and the resulting mixture was refluxed for 4 h, and then the lower boiling components were distilled off from the mixture. The residue was further distilled at reduced pressure to give 7.19 g (0.029 mol) G0. (Yield: 58%). b.p. 136–142 °C at 11.5mmHg. $^1$H NMR ($CDCl_3$): $\delta$ (ppm) 0.03 (s, 12H, $SiCH_3$), 0.45–0.50 (t, 4H, $SiCH_2CH_2CH_2NH_2$), 1.37–1.47 (m, 8H, $SiCH_2CH_2CH_2NH_2$), 2.61–2.66 (m, 4H, $SiCH_2CH_2CH_2NH_2$).

### 2.5. Preparation of G0.5

According to the procedure described in Scheme 1, G0.5 was prepared by two different strategies.

*Method one*: A suspension of 1.34 g (5.40 mmol) G0, 3.72 g (43.20 mmol) MA and 50 ml of methanol was stirred under argon atmosphere at 50 °C for about 2d. Then the solvent and excess MA was removed under reduced pressure at 50 °C using a rotary evaporator, and 3.06 g (5.16 mmol) G0.5 was obtained. (Yield: 95%).

*Method two*: A suspension of 5.50 g (0.024 mol) DMAA and three drops of Karstedt catalyst was added into the flask, and then 1.34 g (0.01 mol) $M^HM^H$ was added dropwise with stirring. The reaction was carried out under argon atmosphere at 70 °C for 48 h. After the reaction completed, the solvent and excess DMAA were removed under reduced pressure using a rotary evaporator. To ensure the complete evaporation of DMAA, the product was redissolved in methanol and removed under reduced pressure again, 5.46 g (9.22 mmol) G0.5 was obtained. (Yield: 92%). $^1$H NMR ($CDCl_3$): $\delta$ (ppm) 0.02 (s, 12H, $SiCH_3$), 0.41 (t, 4H, $SiCH_2CH_2CH_2N$), 1.33–1.44 (m, 4H, $SiCH_2CH_2CH_2N$), 2.34–2.44 (m, 12H, $SiCH_2CH_2CH_2NCH_2$), 2.74 (t, 8H, $NCH_2CH_2CO$), 3.63 (s, 12H, $OCH_3$). $^{13}$C NMR ($CDCl_3$): $\delta$ (ppm) 0.32, 15.77, 20.88, 32.51, 49.26, 51.46, 57.19, 172.97. LC/MS: $m/z$ 593.9 $[M]^+$ (calcd. 592.9).

### 2.6. Preparation of G1.0

A solution of 1.18 g (1.99 mmol) G0.5, 12 g (200 mmol) EDA and 50 ml methanol was stirred under argon atmosphere at 50 °C for about 3d. Then the solvent was removed under reduced pressure at 50 °C using a rotary evaporator. The excess EDA was removed using an azeotropic mixture of toluene and methanol ($v/v$ = 9:1). The remaining toluene was removed by azeotropic distillation using methanol. Finally, 1.38 g (1.96 mmol) G1.0 was obtained. (Yield: 98%). $^1$H NMR ($CDCl_3$): $\delta$ (ppm) 0.04 (s, 12H, $SiCH_3$), 0.41 (t, 4H, $SiCH_2CH_2CH_2N$), 1.38–1.46 (m, 4H, $SiCH_2CH_2CH_2N$), 1.88 (s, 8H, $NH_2$), 2.36 (t, 8H, $NCH_2CH_2CO$), 2.42 (t, 4H, $SiCH_2CH_2CH_2N$), 2.71 (t, 8H, $NCH_2CH_2CO$), 2.82 (t, 8H, $NCH_2CH_2NH_2$), 3.25–3.31(m, 8H, $NCH_2CH_2NH_2$), 7.66 (t, 4H, CONH). $^{13}$C NMR ($CDCl_3$): $\delta$ (ppm) 0.31, 15.95, 20.12, 33.83, 41.19, 41.90, 49.85, 56.75, 172.92. LC/MS: $m/z$ 706.0 $[M]^+$ (calcd. 705.1).

### 2.7. Preparation of G1.5

A suspension of 0.98 g (1.39 mmol) G1.0, 3.84 g (44.6 mmol) MA and 50 ml of methanol was stirred under argon atmosphere at 50 °C for about 3d. Then the solvent and excess MA was removed under reduced pressure at 50 °C using a rotary evaporator. The product was redissolved in methanol and redistilled by rotary evaporator again, 1.86 g (1.33 mmol) G1.5 was obtained. (Yield: 96%). $^1$H NMR ($CDCl_3$): $\delta$ (ppm) 0.04 (s, 12H, $SiCH_3$), 0.42 (t, 4H, $SiCH_2CH_2CH_2N$), 1.43–1.47 (m, 4H, $SiCH_2CH_2CH_2N$), 2.37–2.48(m, 24H, $NCH_2CH_2CO$), 2.53 (t, 12H, $CH_2NCH_2$), 2.74–2.80 (m, 24H, $NCH_2CH_2CO$), 3.28–3.29 (m, 8H, $CONHCH_2CH_2NCH_2$), 3.67 (s, 24H, $OCH_3$), 7.19–7.21 (m, 4H, CONH). $^{13}$C NMR ($CDCl_3$): $\delta$ (ppm) 0.28, 15.85, 20.00, 32.51, 37.03, 49.41, 50.19, 51.45, 52.11, 52.87, 56.53, 172.21, 172.94. LC/MS: $m/z$ 1394.2 $[M]^+$ (calcd. 1393.8).

### 2.8. Preparation of G2.0

Under argon atmosphere, a solution of 0.80 g (0.57 mmol) G1.5, 4.32 g (72 mmol) EDA and 50 ml methanol was stirred at 50 °C for about 6d. After the reaction is complete, the purification procedures were similar to that of G1.0. Afterward, 0.87 g (0.54 mmol) G2.0 was obtained. (Yield: 95%). $^1$H NMR ($CDCl_3$): $\delta$ (ppm) 0.03 (s, 12H, $SiCH_3$), 0.38 (t, 4H, $SiCH_2CH_2CH_2N$), 1.36–1.44 (m, 4H, $SiCH_2CH_2CH_2N$), 2.30 (s, 16H, $NH_2$), 2.39–2.48 (m, 24H, $NCH_2CH_2CO$), 2.69–2.78 (m, 28H, $SiCH_2CH_2CH_2N$, $NCH_2CH_2CO$), 2.83–2.94 (m, 24H, $NCH_2CH_2N$), 3.31–3.23(m, 24H, $NCH_2CH_2NH_2$), 3.62 (s, 3H, $OCH_3$), 7.85–7.92 (m, 12H, CONH). $^{13}$C NMR ($CDCl_3$): $\delta$ (ppm) 0.24, 15.60, 19.87, 32.07, 34.05, 37.50, 41.21, 42.06, 44.25, 49.45, 51.62, 52.68, 56.57, 172.92, 173.22. LC/MS: $m/z$ 1590.9 $[M]^+$ (calcd. 1590.2).

### 2.9. Preparation and luminescent properties of siloxane-based PAMAM dendrimers–lanthanide complexes

The luminescent properties of siloxane-based PAMAM dendrimers–lanthanide complexes were investigated according to the similar procedures described elsewhere [18,36]. A typical procedure is that: Under argon atmosphere, a known amount of G0.5–G2.0 (0.050 mmol) was dissolved in 10 ml dry THF, and a stoichiometric proportion of $Ln(NO_3)_3\cdot 6H_2O$ (Ln = Eu, Tb) was added to the solution. The mixture was stirred and refluxed for 2h. The resulting solution was filtered, and the filtrate was allowed to stand at room temperature for 24h, and then transferred to a quartz cell for optical measurements.

## 3. Results and discussion

### 3.1. Optimization of reaction condition

In general, the synthesis of PAMAM dendrimers based on novel cores was commonly achieved by divergent method through the following steps: (1) Introduction of the amino groups to the core unit. (2) Michael addition of MA to the amino groups. (3) Amidation

of the terminal ester groups with EDA. Then repeat the last two steps in sequence to obtain the following series of products. Based on this idea, G0 was developed as core unit for the construction of the siloxane-based PAMAM dendrimers as shown in Scheme 1. To obtain G0.5, two different approaches were adopted: (1) In method one, the amino groups were firstly introduced to the core unit via the hydrosilylation of ATMS with $M^HM^H$ in the presence of karstedt catalyst. Then, Michael addition of MA to the amino groups of the core unit was followed to obtain G0.5. (2) In method two, the reaction precursor DMAA was firstly synthesized by the Michael addition reaction of MA with AA. Then G0.5 was obtained by the hydrosilylation of DMAA with $M^HM^H$ in the presence of karstedt catalyst. In the first method, hydrosilylation of ATMS with $M^HM^H$, and the subsequent alcoholysis to give the key starting material G0 in 58% yield. It is noticeable that during the reaction process, the amino group of AA should be protected by trimethylsilyl groups to reduce the side-reaction between amino group and the Si–H bond [34]. Furthermore, ATMS must be added in excess to ensure the complete reaction with $M^HM^H$ due to its relative lower activity. To overcome this drawback and the tedious protection-deprotection procedures, method two was developed. In method two, DMAA was obtained by the Michael addition of MA with AA at 50 °C for 36h in nearly 100% yield. Then, hydrosilylation of DMAA with $M^HM^H$ in the presence of karstedt catalyst at relatively lower temperature (70 °C) for 48h to obtained G0.5 in higher yield (92%). Then, G1.0–G2.0 was synthesized by the divergent method following the alternate amidation and Michael addition reactions. Due to its simple synthetic procedures and much higher yield, method two was more suitable for the synthesis of siloxane-based PAMAM dendrimers.

### 3.2. The characterization of siloxane-based PAMAM dendrimers

The structures of the compounds were characterized by FTIR, $^1$H NMR, $^{13}$C NMR, LC/MS, and the thermal properties of the dendrimers were evaluated by DSC and TGA. Fig. 1 shows the FTIR spectra of $M^HM^H$, DMAA, and G0–G2.0. For $M^HM^H$, a characteristic band at 2110 $cm^{-1}$ corresponding to υ(Si–H) and intense bands near 1251 $cm^{-1}$ attributed to δ(Si–$CH_3$) were observed. After the hydrosilylation reaction of $M^HM^H$ with ATMS, the vibration peak at 2110 $cm^{-1}$ for υ(Si–H) disappears in FTIR spectrum of G0, while the vibration peak at 1251 $cm^{-1}$ for δ(Si–$CH_3$) can still be observed. Furthermore, the new adsorption peaks at 3292 $cm^{-1}$, 3366 $cm^{-1}$, and 1598 $cm^{-1}$ corresponding to υ($NH_2$) and δ($NH_2$) were observed, suggested that the amino groups were successfully introduced to the core unit. For ester-terminated siloxane-based PAMAM dendrimers G0.5 and G1.5, the adsorption at 1735 $cm^{-1}$ suggested the presence of ester group (–$CO_2CH_3$), while the amino-terminated products G1.0 and G2.0 present the typical amino group ($NH_2$) adsorption peaks at 3286 $cm^{-1}$, 3317 $cm^{-1}$, and 1640 $cm^{-1}$. In the convergent method for the synthesis of G0.5, the hydrosilylation reaction can also be monitored by the disappearance of vibration peak at 2110 $cm^{-1}$ and 3070 $cm^{-1}$ for υ(Si–H) and υ(C=C), and the appearance of ester bonds (–$CO_2CH_3$) adsorption peaks at 1735 $cm^{-1}$.

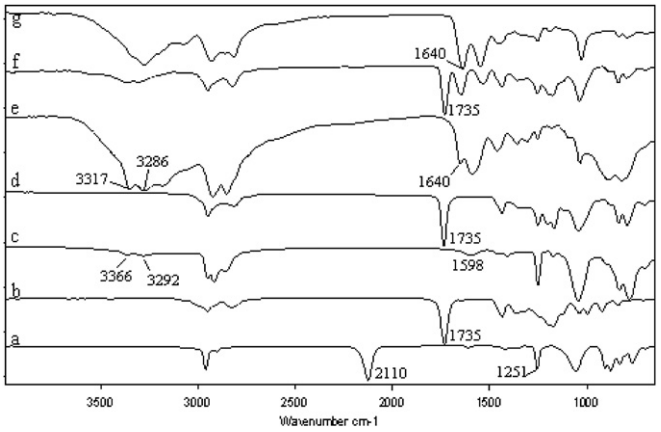


**Fig. 1.** FTIR spectra of $M^HM^H$, DMAA, and siloxane-based PAMAM dendrimers. (a) $M^HM^H$ (b) DMAA (c) G0 (d) G0.5 (e) G1.0 (f) G1.5 (g) G2.0.

The $^1$H NMR of DMAA exhibits the characteristic resonances for allyl protons in the region of 5.07–5.15 and 5.70–5.80 ppm, and for ester protons ($OCH_3$) at 3.62 ppm. For G0, Si–C$H_3$ protons exhibit resonances in the region of 0.00–0.07 ppm, while the protons in the region of 1.37–1.47 ppm attributed to the protons of amino groups. The $^1$H NMR spectrum of G0.5 exhibits resonances for Si–C$H_3$ protons between −0.01 and 0.07 ppm and for ester protons ($OCH_3$) at 3.63 ppm. The $^1$H NMR spectrum of G1.5 is almost identical to that of G0.5 for analogous protons, although broader resonances are observed with the increasing generation. The reason for this can be ascribed to the slightly different chemical environments for the protons in different generations and the restricted mobility of the respective protons in the outer shells [37,38]. For the amino-terminated product G1.0, the resonances appeared in the range of 0.00–0.08, 1.88, and 7.71–7.75 ppm are corresponding to the protons of Si–C$H_3$, –N$H_2$, and –CON*H*. The $^1$H NMR spectrum of G2.0 exhibits identical resonance patterns to those observed in its counterpart G1.0, although broader signals were observed with increasing generation.

Furthermore, the molecular structures of the siloxane-based PAMAM dendrimers are also proved by $^{13}$C NMR and LC/MS. The spectroscopic data of $^{13}$C NMR are consistent with the assignment obtained by the $^1$H NMR. The molecular weights determined by LC/MS are in well agreement with the theoretical results, further supporting that the desired siloxane-based PAMAM dendrimers have been successfully synthesized.

The incorporation of siloxane on the thermal properties of the resulting PAMAM dendrimers was investigated by DSC and TGA. The glass transition temperature ($T_g$) of G0.5–G2.0 and their corresponding amino-terminated products using EDA as core molecular were present in Table 1. As shown in Table 1, the siloxane-based PAMAM dendrimers all possess low $T_g$ values. The $T_g$ values for the ester-terminated products G0.5 and G1.5 are −83.52 °C and −52.76 °C, respectively. The $T_g$ values of the amino-terminated products G1.0 and G2.0 are −59.45 °C and −3 °C, which are lower than those of the corresponding EDA-cored PAMAM [39]. The low $T_g$ values of siloxane-based dendrimers indicate that the introduction of siloxane into the interior of the dendrimer has greatly improve the flexibility of dendrimer structures, and would alleviate the surface congestion of high generation products.

Fig. 2 shows the TGA curves of the dendrimers in nitrogen atmosphere. As can be seen from Fig. 2, the ester-terminated

**Table 1**
Glass transition temperature ($T_g$) of siloxane-based PAMAM dendrimers and EDA-cored PAMAM dendrimers.

| Dendrimers | $T_g$ |
|---|---|
| G0.5 | −83.52 |
| G1.0 | −59.45 |
| G1.5 | −52.76 |
| G2.0 | −3.21 |
| EDA–G1.0[a] | −3 |
| EDA–G2.0[a] | 0 |

[a] Cited from Ref. [39].

products G0.5 and G1.5 are thermally stable when the temperature below 200 °C. The amino-terminated products G1.0 and G2.0 show relatively low thermal stability, and began to decompose at the start of heating. The TGA curves of G1.0 and G2.0 indicate two major weight loss stages. For the first stage, the maximum rate of weight loss occurs around 120 °C, corresponding to the residual solvent and EDA encapsulated in the amino-terminated products. The formation of hydrogen bond between the amino groups leading to the viscosity increased in G1.0 and G2.0, which made it hard for the completely removal of methanol and EDA, and thus the first stage occurred. The second stage accounts for the decomposition of the dendrimer structures with the maximum rate occurs around 250 °C similar to their counterparts using EDA as the core unit in the previous study [39,40].

### 3.3. Luminescent properties of siloxane-based PAMAM dendrimers–lanthanide complexes

The luminescent properties of siloxane-based PAMAM dendrimers–lanthanide complexes were investigated in THF solution at room temperature. Figs. 3 and 4 show the excitation and emission spectra of the dendrimers complexes with Eu(III).

The excitation spectra of these complexes were all obtained by monitoring the emission peak of Eu(III) at 617 nm. As can be noticed in Fig. 3, broad excitation bands located at 350–400 nm can be found for all the complexes and 395 nm is the most appropriate excitation band. As can be seen from the emission spectra in Fig. 4, the intense narrow band located at 617 nm corresponding to the hypersensitive $^5D_0 \rightarrow {}^7F_2$ transition of Eu(III) ion was found for the complexes of G0.5, G1.5, and G2.0. The presence of bands at 593 nm, 650 nm and 688 nm associated with the characteristic transitions of $^5D_0 \rightarrow {}^7F_1$, $^5D_0 \rightarrow {}^7F_3$ and $^5D_0 \rightarrow {}^7F_4$, respectively. The transitions of $^5D_0 \rightarrow {}^7F_0$ at 580 nm could not be observed for all the cases, which means no inverse center for Eu(III) ion in those complexes [18,41]. It is known that the $^5D_0 \rightarrow {}^7F_2$ transition induced by the electric dipole moment is very sensitive to the coordination environment of the Eu(III) ion, while the $^5D_0 \rightarrow {}^7F_1$ transition arose from the magnetic dipole is less sensitive to the coordination environment. Thus, the emission spectra were normalized with respect to the $^5D_0 \rightarrow {}^7F_1$ transition [10,36]. The asymmetry factor, which is the ratio of the integrated intensity of $^5D_0 \rightarrow {}^7F_2$ transition to $^5D_0 \rightarrow {}^7F_1$ transition, has been widely used as an indicator of Eu

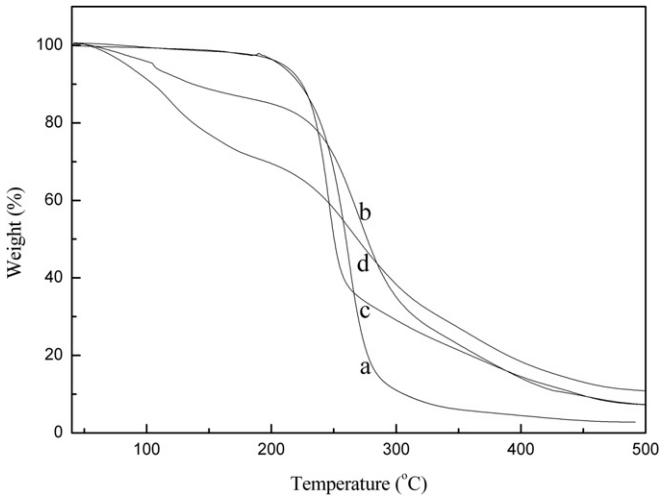


**Fig. 2.** TGA curves of siloxane-based PAMAM dendrimers. (a) G0.5 (b) G1.0 (c) G1.5 (d) G2.0.

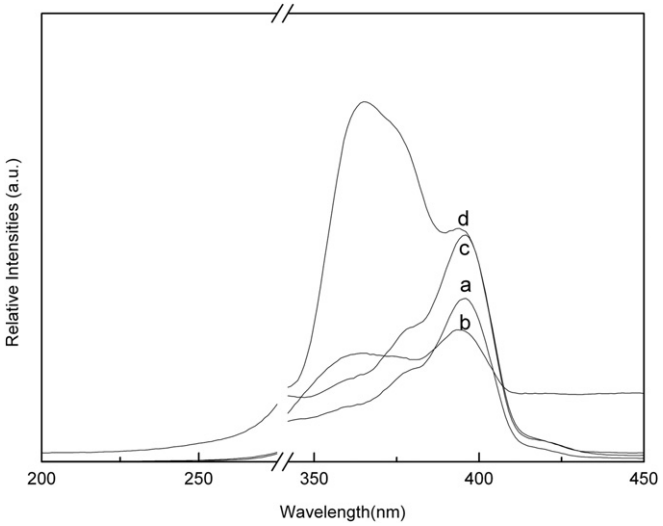


**Fig. 3.** The excitation spectra of siloxane-based PAMAM dendrimers-Eu(III) complexes (a) G0.5 (b) G1.0 (c) G1.5 (d) G2.0.

(III) site symmetry [41]. The asymmetry factor for the complexes of G0.5, G1.5, and G2.0 are 5.6, 6.2, and 5.9, indicating that Eu(III) ion in these complexes has lower symmetric coordination environment. Compared with the complexes of G0.5, G1.0, and G2.0, the luminescent properties of G1.0 with Eu(III) was relatively poor. As is shown in Fig. 4(d), the ligand emission (located at 450–500 nm) intensity was stronger than those of the characteristic Eu(III) ion emission. The reason for this might be that, amino groups of G1.0 also take part in the coordination process with Eu(III), the high energy vibrations of N–H may quench the excited state of Eu(III) ions, resulting in the poor luminescent properties of G1.0 complex [42]. Although G2.0 also contains amino groups at peripheral, there are more carbonyl groups in the interior of G2.0 compared with G1.0. Since the coordination ability of oxygen with lanthanide ions is stronger than that of the nitrogen, the luminescent properties of G2.0 complex were better than that of G1.0 complex [43]. Furthermore, Eu(III) ions can also be encapsulated in the interior of G2.0 structure, while it is hard for G1.0 to encapsulate Eu(III) ions as the early generation dendrimer G1.0 possesses relatively open structure. Another phenomenon can also be observed from Fig. 4, with the increasing of the generation number, the ligand emission located at 450–500 nm nearly vanish in G2.0 complex, indicated that the energy transfer between the ligand and Eu(III) ions tend to be perfect at that generation, further indicating the synthesized dendrimers are promising candidate for luminescent materials.

The emission spectra of Tb(III) complexes with G0.5–G2.0 excited at 250 nm were recorded in Fig. 5. The emission spectra of the Tb(III) complexes with G0.5, G1.5 and G2.0 exhibit the characteristic narrow-width emission bands, which were related to the transition from the triplet state energy level of Tb(III) to different single state levels and were assigned to the $^5D_4 \rightarrow {}^7F_6$ (487 nm), $^5D_4 \rightarrow {}^7F_5$ (545 nm), $^5D_4 \rightarrow {}^7F_4$ (585 nm), and $^5D_4 \rightarrow {}^7F_3$ (620 nm) transitions. Compared with the other complexes, the complex of G1.0 exhibits poor luminescent properties, as weaker emission peaks corresponding to characteristic emission bands of Tb(III) ions and stronger emission peaks belong to the ligand were observed. The reason for this was similar to that of its Eu (III) complex. It is noteworthy that the ligand emission background in the region 400–450 nm nearly could not be detected in the emission spectra of these complexes with the generation number increasing from G0.5, G1.5 to G2.0, indicated that the energy transfer between the higher generation dendrimer and Tb (III) ions is more efficient. A

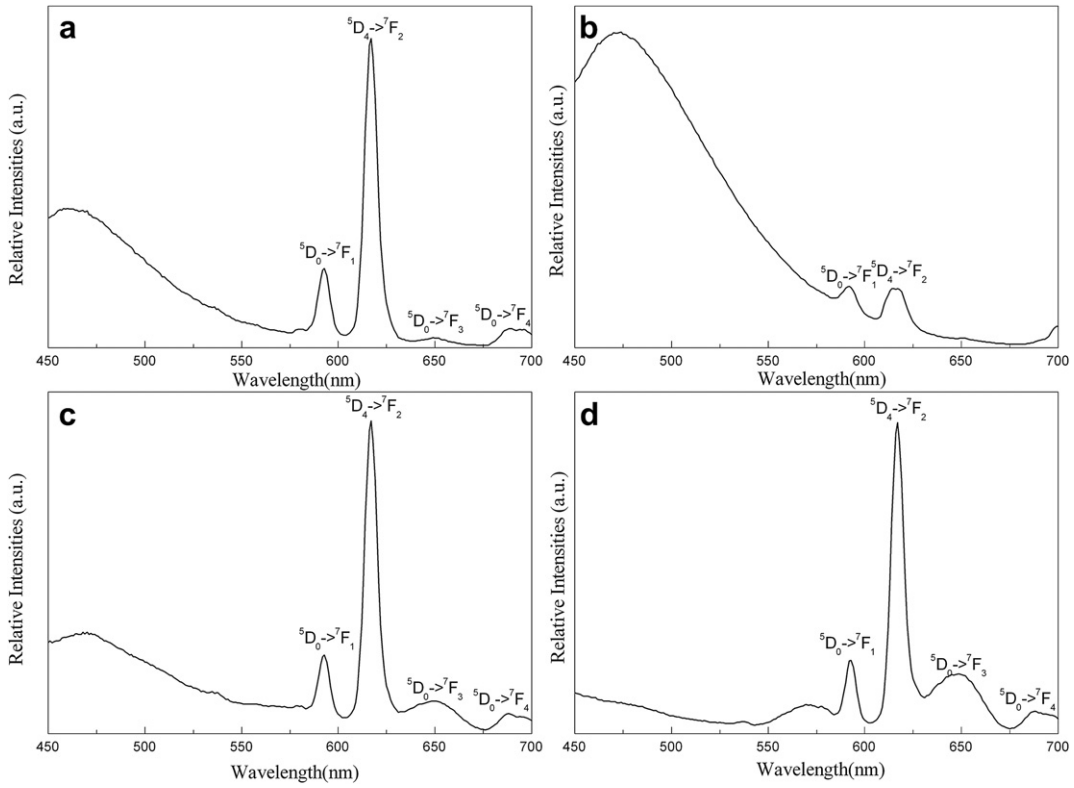


**Fig. 4.** The emission spectra of siloxane-based PAMAM dendrimers-Eu(III) complexes ($\lambda_{ex}$ = 395 nm) (a) G0.5 (b) G1.0 (c) G1.5 (d) G2.0.

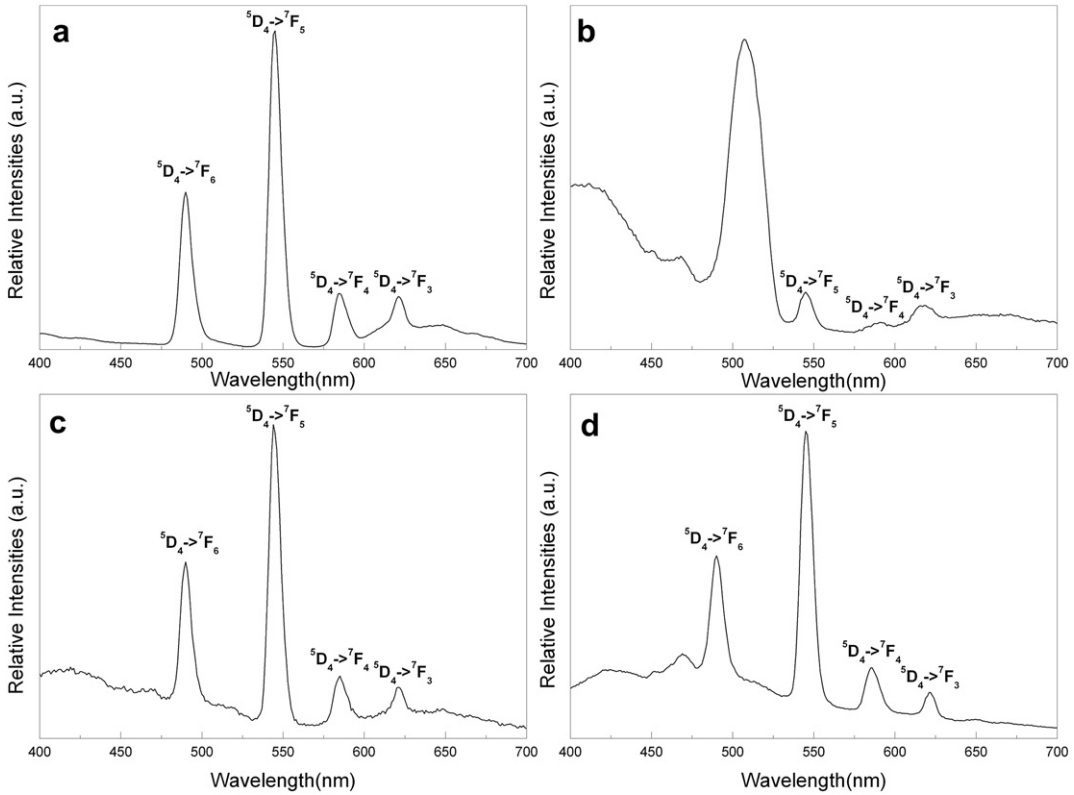


**Fig. 5.** The emission spectra of siloxane-based PAMAM dendrimers-Tb(III) complexes ($\lambda_{ex}$ = 250 nm) (a) G0.5 (b) G1.0 (c) G1.5 (d) G2.0.

reasonable explanation for this is that: the binding ability of G0.5–G2.0, which is mainly due to the functional groups, increased with the increasing generation; furthermore, the number of interior cavities is also increased with increasing generation number, since the metal ions can be easily encapsulated within the cavities, the binding ability of dendrimer also increased.

## 4. Conclusions

In conclusion, the 0.5–2 generations of siloxane-based PAMAM dendrimers with 1,3-bis(3-aminopropyl) tetramethyldisiloxane (G0) as core unit were prepared via two different methods. Results indicate that method two is more suitable for the synthesis of the dendrimers for its simple synthetic procedure and higher yield. DSC analysis shows that the introduction of the siloxane into the interior of the dendrimers has great effect on the flexibility of the dendrimer structures as evidenced by DSC analysis. Except for G1.0, narrow-width red and green emissions were observed for the complexes of G0.5, G1.5, and G2.0 with Eu(III) and Tb(III), indicating intramolecular energy transfer process takes place between the lanthanide ions and the ligands. The improved structure flexibility and surface congestion after the incorporation of siloxane not only make it easy for the metal ions to diffuse into the interior of the dendrimer structures, but also the provide the possibility to synthesize the higher generation dendrimers or peripherally functionalize the dendrimers with certain groups according to the applications.

## Acknowledgements

The authors are grateful for the financial support by the National Natural Science Foundation of China (No. 20574043 and 20874057), the China Postdoctoral Science Foundation Funded Project (2008041135), and the Key Natural Science Foundation of Shandong Province (Z2007B02). The authors are also grateful to the editor and the reviewers for their valuable comments and constructive suggestions

## References

[1] N. Sabbatini, M. Guardigli, J.M. Lehn, Coord. Chem. Rev. 123 (1993) 201–228.
[2] D. Parker, R.S. Dickins, H. Puschmann, C. Crossland, J.A.K. Howard, Chem. Rev. 102 (2002) 1977.
[3] E.G. Moore, A.P.S. Samuel, K.N. Raymond, Acc. Chem. Res. 42 (2009) 542–552.
[4] L. Armelao, S. Quici, F. Barigelletti, G. Accorsi, G. Bottaro, M. Cavazzini, E. Tondello, Coord. Chem. Rev. 254 (2010) 487–505.
[5] N. Weibel, L.J. Charbonnière, M. Guardigli, A. Roda, R. Ziessel, J. Am. Chem. Soc. 126 (2004) 4888–4896.
[6] A. Picot, A. D'Aléo, P.L. Baldeck, A. Grichine, A. Duperray, C. Andraud, O. Maury, J. Am. Chem. Soc. 130 (2008) 1532–1533.
[7] G.L. Law, K.L. Wong, C.W.Y. Man, W.T. Wong, S.W. Tsao, M.H.W. Lam, P.K.S. Lam, J. Am. Chem. Soc. 130 (2008) 3714–3715.
[8] J. Hynes, T.C. O'Riordan, A.V. Zhdanov, G. Uray, Y. Will, D.B. Papkovsky, Anal. Biochem. 390 (2009) 21–28.
[9] M. Elbanowski, B.M. Kowska, J. Photochem. Photobiolo. A 99 (1996) 85–92.
[10] J.P. Cross, M. Lauz, P.D. Badger, S. Petoud, J. Am. Chem. Soc. 126 (2004) 16278–16279.
[11] C.P. Montgomery, B.S. Murray, E.J. New, R. Pal, D. Parker, Acc. Chem. Res. 42 (2009) 925–937.
[12] J.M. Lehn, Angew. Chem. Int. Edit 29 (1990) 1177–1370.
[13] D. Dong, S. Jiang, Y. Men, X. Ji, B. Jiang, Adv. Mater. 12 (2000) 646–649.
[14] Y.T. Yang, S.Y. Zhang, Acta A 60 (2004) 2065–2069.
[15] N. Arnaud, J. Georges, Spectrochim. Acta A 59 (2003) 1829–1840.
[16] J.G. Bünzli, C. Piguet, Chem. Soc. Rev. 34 (2005) 1048–1077.
[17] X.F. Wen, M.Y. Li, Y. Wang, J.P. Zhang, L.M. Fu, R. Hao, Y. Ma, X.C. Ai, Langmuir 24 (2008) 6932–6936.
[18] L. Liu, H.F. Lu, H. Wang, Y.L. Bei, S.Y. Feng, Appl. Organomet. Chem. 23 (2009) 429–433.
[19] D.A. Tomalia, A.M. Naylor, W.A. Goddard III, Angew. Chem. Int. Edit 29 (1990) 138–175.
[20] A.W. Bosman, H.M. Janssen, E.W. Meijer, Chem. Rev. 99 (1999) 1665–1688.
[21] S.M. Grayson, J.M.J. Fréchet, Chem. Rev. 101 (2001) 3819–3868.
[22] G.R. Newkome, C.D. Shreiner, Polymer 49 (2008) 1–173.
[23] R. Esfanda, D.A. Tomalia, Drug Discov. Today 6 (2001) 427–436.
[24] D. Luo, K. Haverstick, N. Belcheva, E. Han, W.M. Saltzman, Macromolecules 35 (2002) 3456–3462.
[25] M.K. Calabretta, A. Kumar, A.M. McDermott, C.Z. Cai, Biomacromolecules 8 (2007) 1807–1811.
[26] S.H. Medina, M.E.H. El-Sayed, Chem. Rev. 109 (2009) 3141–3157.
[27] R.J. Qu, Y.Z. Niu, C.M. Sun, C.J. Ji, C.H. Wang, G.X. Cheng, Micropor. Mesopor. Mat 97 (2006) 58–65.
[28] R.J. Qu, Y.Z. Niu, J.H. Liu, C.M. Sun, Y. Zhang, H. Chen, C.N. Ji, React. Funct. Polym. 68 (2008) 1272–1280.
[29] I. Gill, A. Ballesteros, J. Am. Chem. Soc. 120 (1998) 8587–8598.
[30] K. Deguchi, K. Tsuru, T. Hayashi, M. Takaishi, M. Nagahara, S. Nagotani, Y. Sehara, G. Jin, H.Z. Zhang, S. Hayakawa, M. Shoji, M. Miyazaki, A. Osaka, N.H. Huh, K. Abe, J. Cerebr. Blood F. Met 26 (2006) 1263–1273.
[31] D.M.L. Goodgame, P.D. Lickiss, S.J. Rooke, A.J.P. White, D.J. Williams, Inorg. Chim. Acta 343 (2003) 61–73.
[32] Y. Abe, T. Gunji, Prog. Polym. Sci. 29 (2004) 149–182.
[33] J.L. Speier, R. Zimmerman, J.S. Webster, J. Am. Chem. Soc. 78 (1956) 2278–2281.
[34] C.F. Li, D.X. Li, S.Y. Feng, Polym. Int. 54 (2004) 1041–1046.
[35] J. Saam, J. Speier, J. Org. Chem. 24 (1959) 119–120.
[36] Z.H. Zhang, Y. Song, T. Okamura, Y. Hasegawa, W.Y. Sun, N. Ueyama, Inorg. Chem. 45 (2006) 2896–2902.
[37] P. Ortega, J.F. Bermejo, L. Chonco, E. Jesus, F. Javier de la Mata, G. Fernández, J.C. Flores, R. Gómez, M.J. Serramía, M.A. Muñoz-Fernandez, Eur. J. Inorg. Chem. 2006 (2006) 1388–1396.
[38] K. Lorenz, R. Muelhaupt, H. Frey, U. Rapp, F.J. Mayer-Posner, Macromolecules 28 (1995) 6657–6661.
[39] H.M. Tan, Y.J. Luo, Dendritic Polymer. Chemical Industry Press, Beijing, 2002, pp. 199–201.
[40] P. Zheng, L.X. Gao, X.G. Sun, S.G. Mei, Iran. Polym. J. 18 (2009) 257–264.
[41] S. Samikkanu, K. Mellem, M. Berry, P.S. May, Inorg. Chem. 46 (2007) 7121–7128.
[42] G.R. Choppin, D.R. Peterman, Coord. Chem. Rev. 174 (1998) 283–299.
[43] Y. Li, B. Yan, H. Yang, J. Phys. Chem. C 112 (2008) 3959–3968.